Electronic Supplementary Material (ESI) for Journal of Materials Chemistry C.

Supplementary Information

Printable Multi-Stage Variable Stiffness Material Enabled by Low Melting Point Particles Additives

Fei Long[a, b, d, f], Yingchun Shao[a], Zihui Zhao[a], Mingquan Fang[a], Zhiyu Zhang[d], Jianjun Guo[a], Aihua Sun[a], Yong Ren[c, d, e, f*], Yuchuan Cheng[a,b*], Gaojie Xu[a]

List of Contents

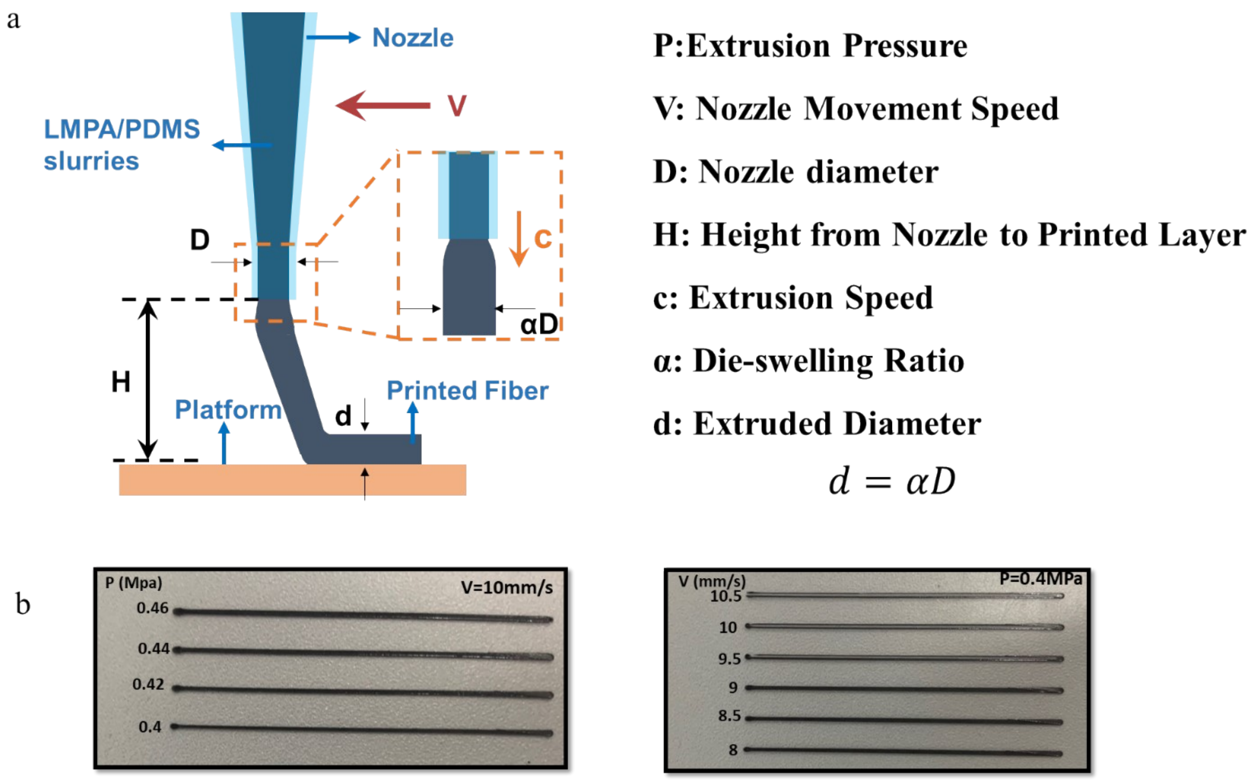

Figure S1. a. Schematic illustration of typical parameters for 3D DIW printing b. The testing printing with different pressure and different velocity.

In the process of 3D DIW, the typical parameters for fiber formation and extruded fiber deposition as shown in Figure S1. Under the action of a certain pressure P, the slurries will be extruded out of the nozzle with the diameter D at a speed c. As most slurries are viscoelastic, die-swelling will take place after extruding from needle with the printer fiber d equaling to αD. Additionally, die-swelling ratio α is relevant to the needle shape and slurries properties [1], which seems hard to predict α in a direct way. Here, test splines (Figure S1b) have been established to select the suitable pressure P and nozzle movement speed V.

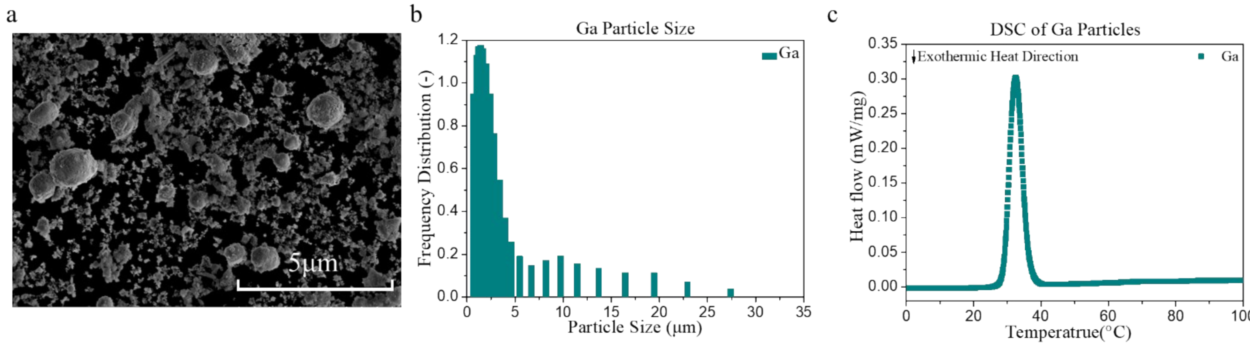

Figure S2. The characterization of Ga a) Morphology by SEM b) Particle Size Distribution c) DCS results of Ga micro-particles

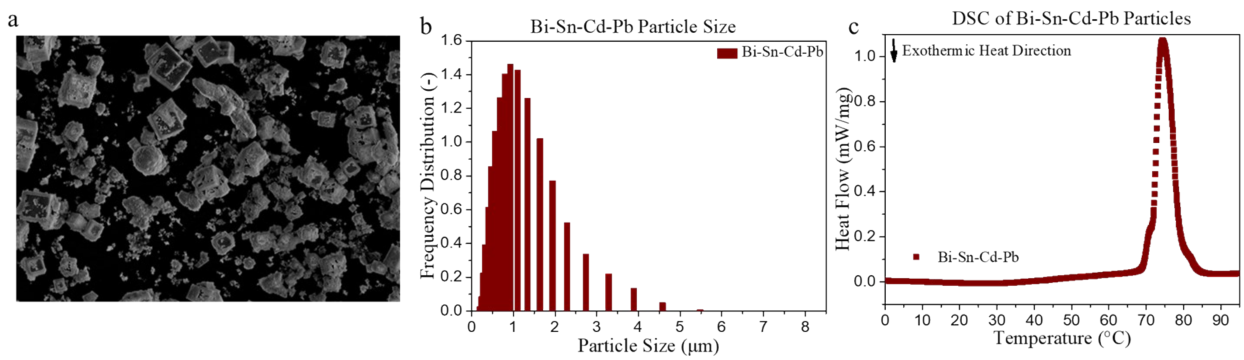

Figure S3. The characterization of Bi-Sn-Cd-Pb a) Morphology by SEM b) Particle Size Distribution c) DCS results of Bi-Sn-Cd-Pb micro-particles.

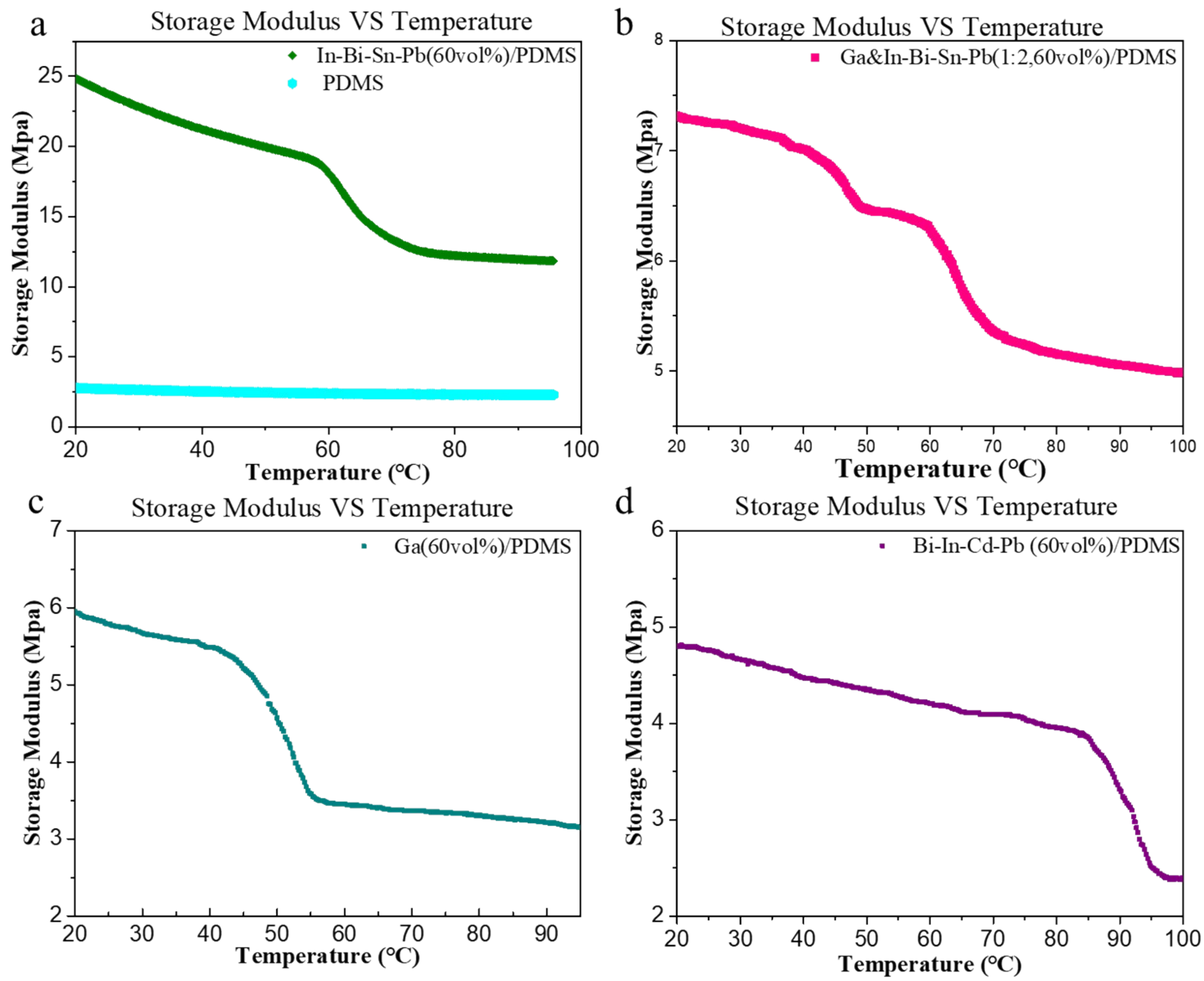

Figure S4. Storage modulus as measured in the DMA versus temperature for a) The comparison of In-Bi-Sn-Pb (60vol%.)/PDMS elastomer with pure PDMS elastomer b) Ga& In-Bi-Sn-Pb (with ratio 1:1 in volume) LMPA/PDMS elastomers. c) Ga/PDMS elastomers. d. Bi-In-Cd-Pb/PDMS elastomers.

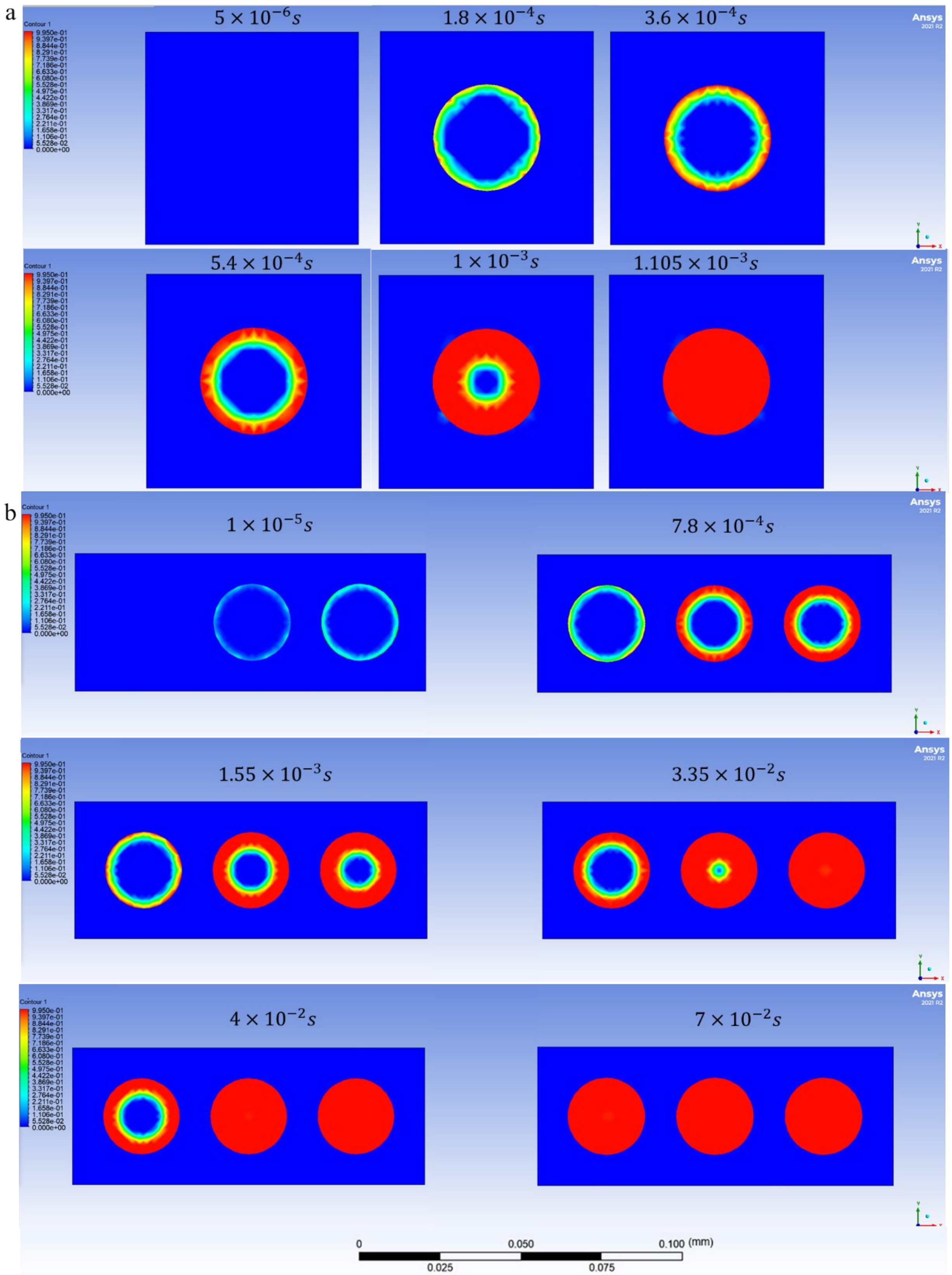

Figure S5. The finite volume method-based simulation results of LMPA melting process from solid phase represented by dark blue color to liquid phase represented by dark red color for a) single LMPA particle, and b) triple LMPA particles.

The numerical approach makes it possible to calculate the melting process that involves conduction process in the solid phase PCM and the convection process in the liquid phase PCM in a simultaneous way. In order to numerically study the melting process of LMPA in PDMS SE 1700, the solidification and melting" model has been used where an enthalpy-porosity technique [1] has been applied to track the change of quantity of liquid phase fraction. Based on enthalpy balance, liquid fraction has been computed in each iteration. Therefore, the governing equation for this melting problem is written as

$$\frac{\partial}{\partial t}(\rho H) + \nabla \cdot (\rho \vec{v} H) = \nabla \cdot (k \nabla T) + S$$

where H is enthalpy, ρ is density, $\vec{v}$ is fluid velocity and S is source term.

In the present investigation, we explore details of LMPA melting process in the mixture of PDMS elastomers. In the initial state, the solid PCM were present adopting spherical shape in PDMS elastomer that can be considered as solid-state during the process due to high melting point around 1700°C. To save the computational cost, the computational domain has been selected such that single-phase transition model with volume of 0.05 mm $\times$ 0.05 mm $\times$ 0.05 mm includes one In-Bi-Sn-Pb microparticle while triple-phase transition model with volume of 0.115 mm $\times$ 0.45 mm $\times$ 0.45 mm involves three types of microparticles. The mesh size has been set with 0.001 and 0.005 mm for single-phase transition and triple-phase transition model, respectively. In the simulation, the initial temperature of the whole system is 27°C. For the PCMs of Ga, In-Bi-Sn-Pb and Bi-Sn-Cd-Pb, the melting interval between 29°C-31°C, 47°C-50°C, 68°C-72°C were applied, respectively, and the other parameters are shown in Table S1.

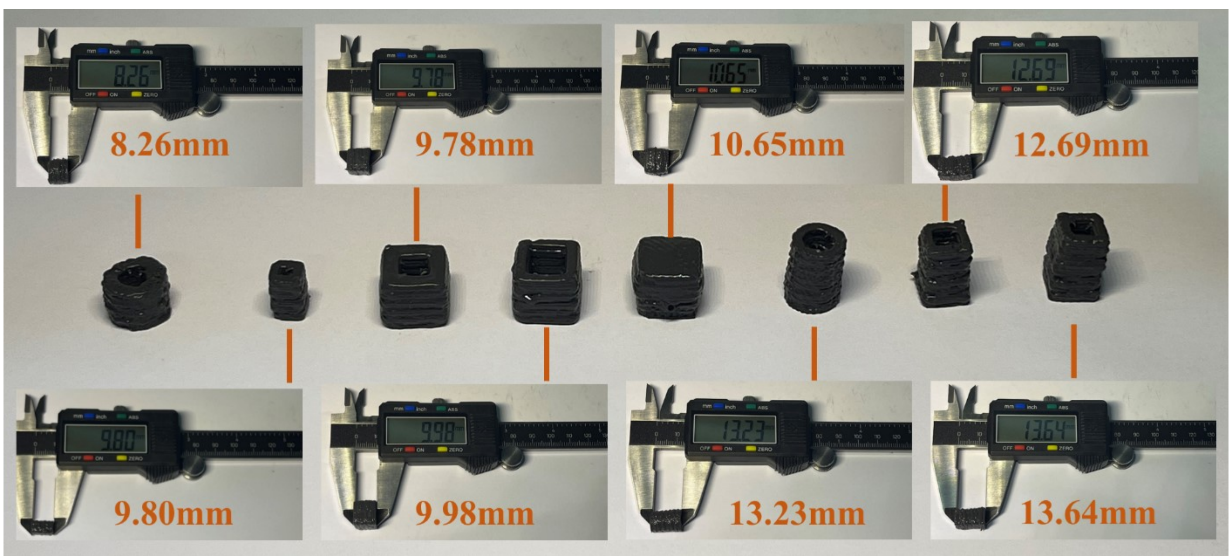

Figure S6. The shapes of cube, hollow cuboid and hollow cylinder fabricated by DIW printing, and the corresponding sample thickness measured by vernier caliper.

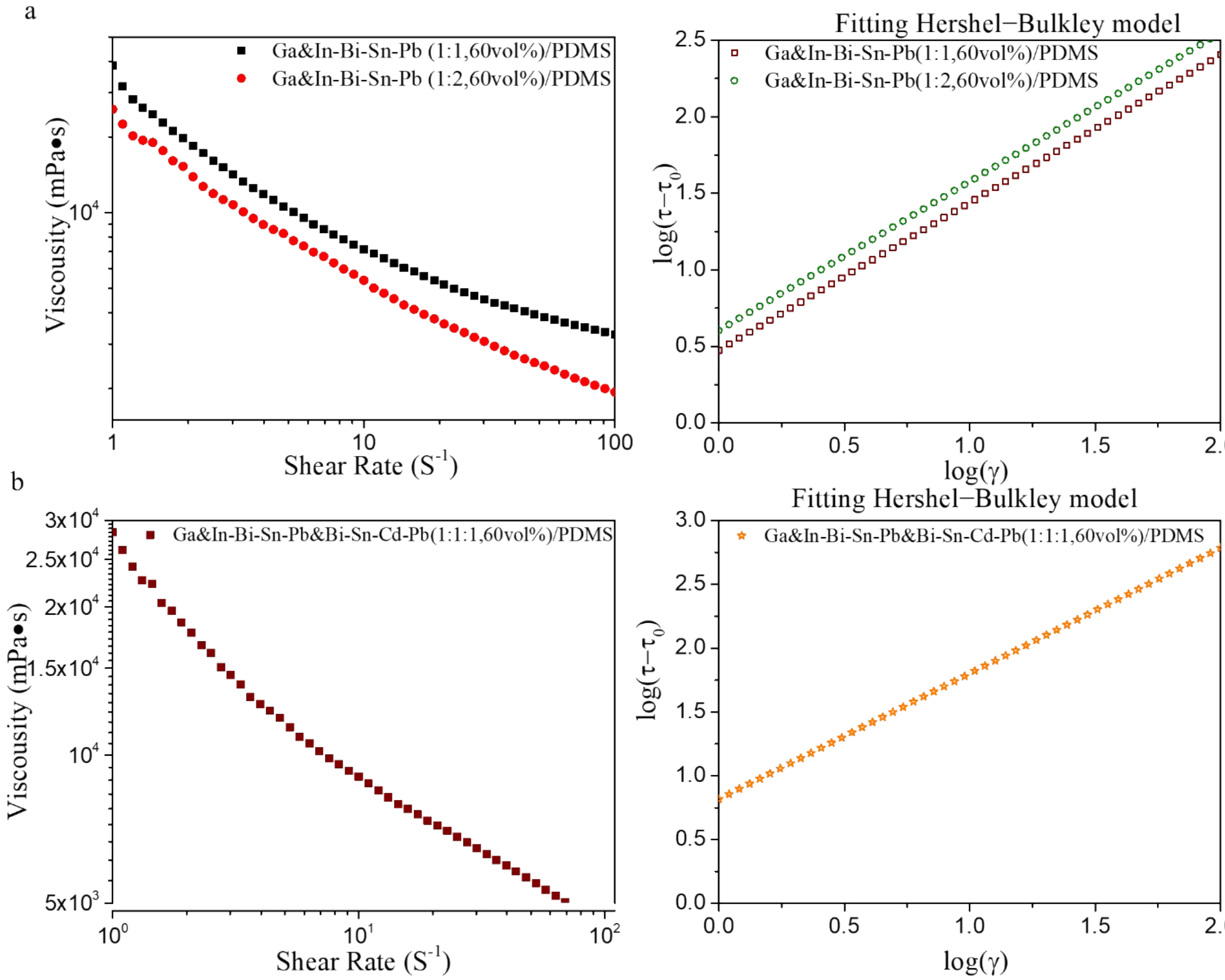

Figure S7. The apparent viscosity as the function of shear rate and fitting Hershel-Bulkey model on the upper right corner for a) Ga&In-Bi-Sn-Pb (1:1,60vol%)/PDMS, b) Ga&In-Bi-Sn-Pb(1:2,60vol%)/PDMS.

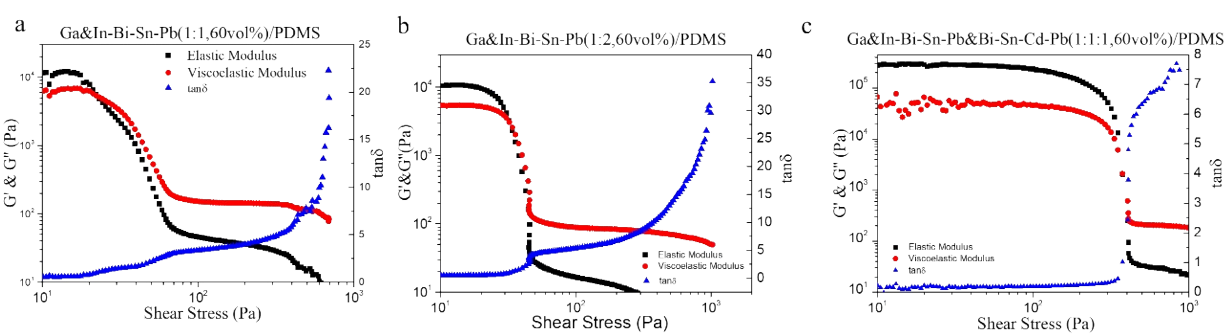

Figure S8. The elastic modulus (G'), viscoelastic modulus (G'') and tanδ for a) Ga&In-Bi-Sn-Pb(1:1,60vol%)/PDMS b) Ga&In-Bi-Sn-Pb(1:2,60vol%)/PDMS c. Ga&In-Bi-Sn-Pb&Bi-Sn-Cd-Pb(1:1:1,60vol%)/PDMS.

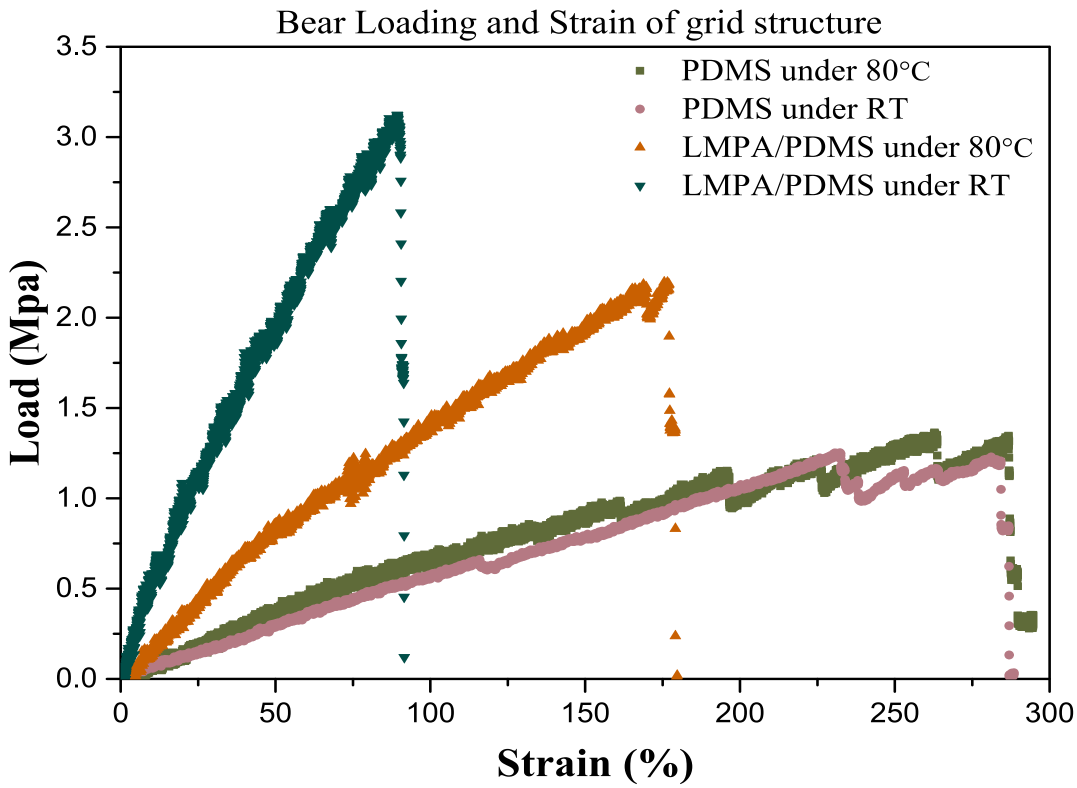

Figure S9. The relationship of bear loading and strain of grid structure

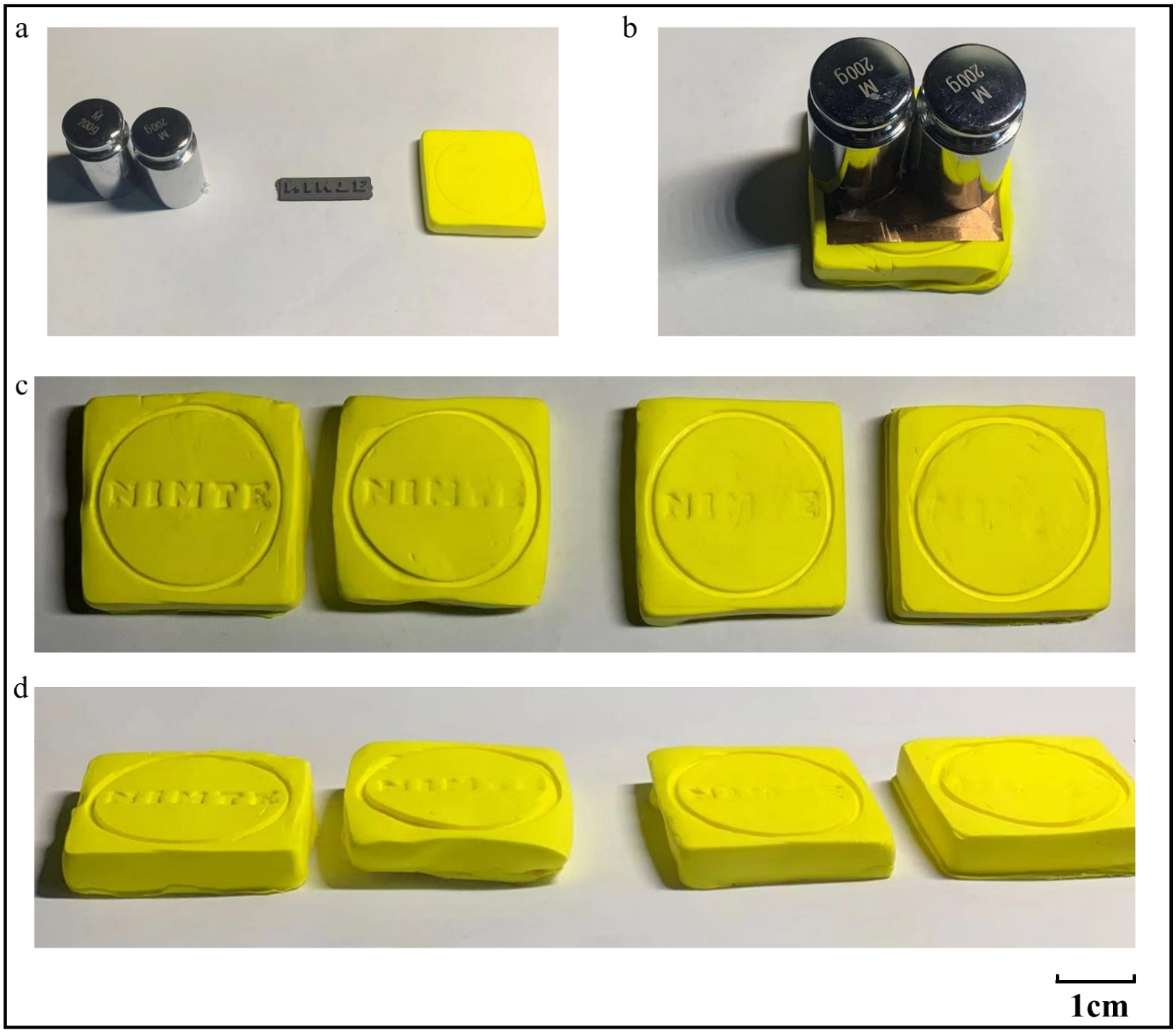

Figure S10. a) Materials for demonstration of controllable stamp. b) Soft actuators under 0.4N load (two 200g weight) c) Front view d. Lateral view.

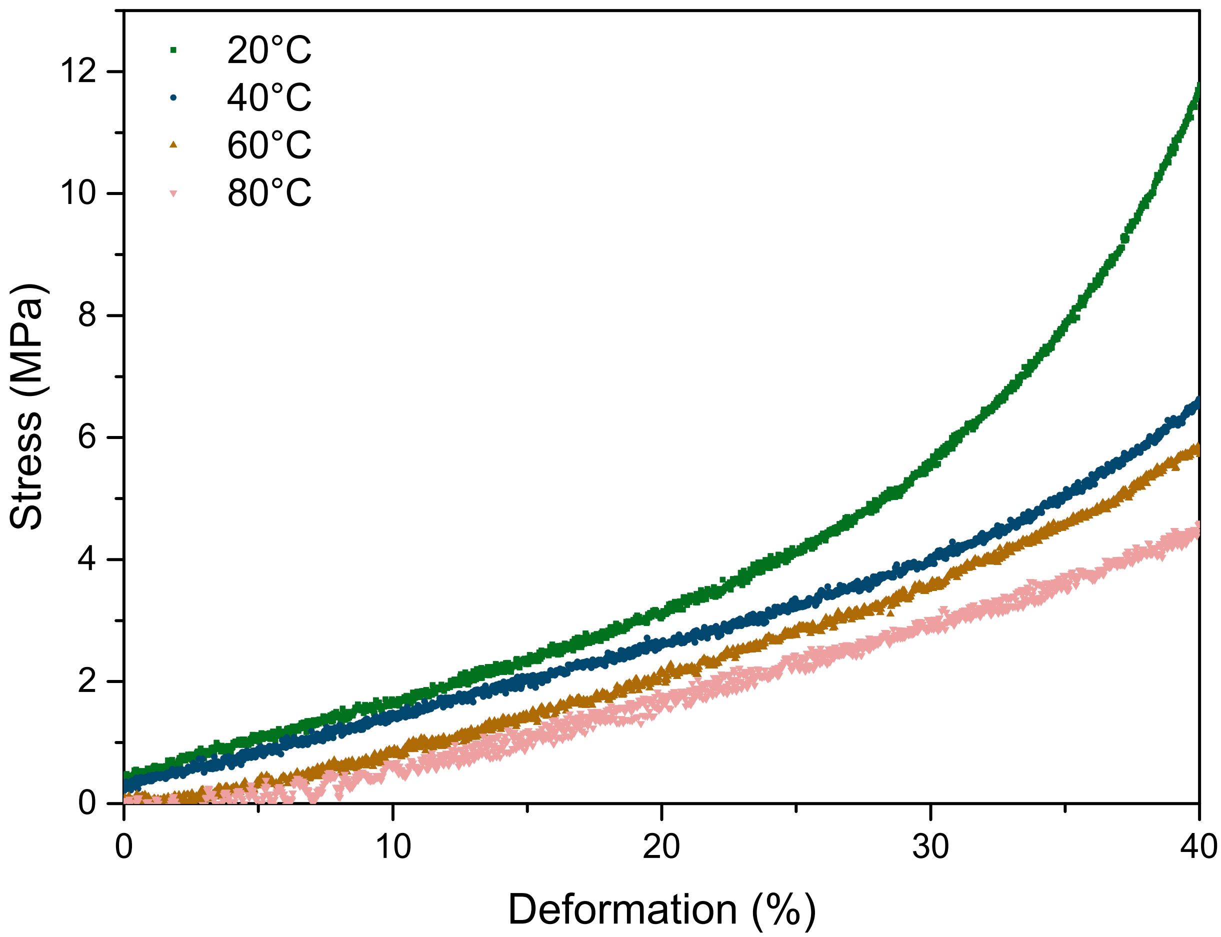

Figure S11 The variation of applied force with temperature

The applied stress of hollow vascular scaffolds with three-legged has been measured by UTM. It was set with the deformation (40%), the applied stress experienced a gradual decrease when the samples were heating from 20℃ to 40℃, 60℃ and 80℃ step by step.

Table S1. The physical properties of materials and the computational set-up in the ANSYS simulation

Physical Properties of Materials			
	Ga	In-Bi-Sn-Pb	Bi-Sn-Cd-Pb
density [kg/m^3]	5907	9160	9670
Cp [J/(kgK)]	109.76	163	146
thermal conductivity [W/(mK)]	29.4	18	18
Viscosity [kg/(ms)]	0.0016	0.0015	0.0015
Computational set-up	single model	triple model	
Number of time steps	50	50000	
Time step size	1.00E-05	1.00E-04	
Max iterations per time step	20	10	

Table S2. The mechanical properties data by Universal Testing Machine

Name	Temperature (℃)	Load (N)	Elongation (%)	Tensile Modulus (Mpa)	Compression Modulus (Mpa)
Ga/PDMS	30	83.7191	38.86856	3.4506	0.60231
	50	78.19970	47.29008	1.81891	0.52204
	80	78.2554	47.49012	1.81686	0.5288
Ga&In-Bi-Sn-Pb(1:1,60vol%)/PDMS	25	88.0323	25.529316	3.82641	0.687
	30	78.4442	28.32927	2.69799	0.61791
	50	71.0226	33.14264	2.10065	0.56882
	80	72.2427	33.76266	2.01485	0.56049
Ga&In-Bi-Sn-Pb&Bi-Sn-Cd-Pb(1:1:1,60vol%)/PDMS	25	83.9522	31.22769	3.30819	0.6098
	30	78.7422	33.82339	3.13627	0.5405
	50	56.6062	36.10925	2.56233	0.47531
	80	48.0304	39.76266	2.26544	0.39279
	100	46.778	39.94224	2.21289	0.38684

Table S3. The primary data in Hershel-Bulker model

Name	τ_0 (Pa)	k(Pa•s^n)	n
In-Bi-Sn-Pb (20vol%)	269.7	30.2	0.87
In-Bi-Sn-Pb (30vol%)	226.9	24.9	0.89
In-Bi-Sn-Pb (40vol%)	127.7	11.7	0.97
In-Bi-Sn-Pb (50vol%)	119.5	9.3	0.98
In-Bi-Sn-Pb (60vol%)	101.5	9.2	0.98
Ga& In-Bi-Sn-Pb (1:1 in 60vol%)	33.9	3.0	0.96
Ga& In-Bi-Sn-Pb (1:2 in 60vol%)	24.3	4.0	0.97
Ga& In-Bi-Sn-Pb& Bi-Sn-Cd-Pb (1:1:1 in 60vol%)	28.4	6.5	0.98

Note: k is consistency index; n is flow index.

Reference List

[1] De Vicente j, (Ed.) Viscoelasticity: From Theory to Biological Applications. BoD–Books on Demand, 2012.

[2] Voller vr, Brent ad, and Reid KJ. Technical report, *Conference for Solidification Processing*, Ranmoor House, Sheffield, September 1987.